Universidade de São Paulo

Biblioteca Digital da Produção Intelectual - BDPI

Departamento de Física e Ciência Interdisciplinar - IFSC/FCI

Artigos e Materiais de Revistas Científicas - IFSC/FCI

2012-07

Spectral editing based on scalar spin-spin interactions: new results on the structure of metathiophosphate glasses
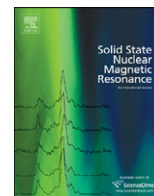
Spectral editing based on scalar spin–spin interactions: New results on the structure of metathiophosphate glasses

Dirk Larink, Jinjun Ren, Hellmut Eckert*

Institut für Physikalische Chemie, WWU Münster, Corrensstrasse 30, D-48149 Münster, Germany

ARTICLE INFO

ABSTRACT

The local structure of glassy $NaPS_3$ and $AgPS_3$ was analyzed based on quantitative ^{31}P MAS-NMR spectroscopy. The glasses contain some oxide impurities, which could be quantified from the NMR spectral analysis. Four discrete resonances are observed in both glasses, which were assigned to four distinct types of phosphate groups $P^{(n)}$, where n is the number of P–S–P bridges(i.e., $P^{(0)}$, $P^{(1)}$, $P^{(2)}$, and $P^{(3)}$ units, respectively) with the help of 2D homonuclear J-resolved and INADEQUATE methods. Based on the results obtained, the interpretations of previous spectra obtained at low spinning speeds on lithium and silver thiophosphate glasses (*Chem. Mater. 2 (1990), 273, and J. Am. Chem. Soc. 114 (1992), 5775*) need to be revised. Contrary to the situation in alkali phosphate glasses, the corresponding sulfide analogs are characterized by a wide $P^{(n)}$ species distribution close to that predicted by a statistical charge distribution. INADEQUATE experiments fail to detect $P^{(n)} - P^{(n-1)}$ connectivities, suggesting that the structure of these glasses is rather inhomogeneous, possibly featuring the different $P^{(n)}$ species in segregated domains.

1. Introduction

^{31}P magic angle spinning (MAS) NMR spectroscopy has been very widely applied towards the structural elucidation of crystalline and glassy phosphates. The success of this technique has been based on the rather facile distinction of the various types of phosphate units having different numbers of bridging oxygen atoms ($P^{(n)}$ species, where n is the number of bridging oxygen atoms) on the basis of their isotropic chemical shifts [1–4]. Consequently, ^{31}P MAS-NMR has become a standard tool for the structural analysis of phosphorus-based glasses [5]. For simple binary alkali phosphate glasses all the results obtained so far have documented convincingly the validity of the so-called "binary" model, in which the types of phosphate species present in a glass of given composition are only those realized in the two crystalline phases bordering the particular composition considered [6,7]. For "stoichiometric" glass compositions corresponding to one of such a crystalline phase only a single type of structural unit is present, which is the one that is featured by this phase. Thus, for instance, the structure of $NaPO_3$ glass is entirely made up of $P^{(2)}$ units with only minimal concentrations of $P^{(1)}$ and $P^{(3)}$ species formed. The situation is less clear for the binary alkali or silver thiophosphate glasses. Previous solid state NMR studies of $Li_2S–P_2S_5$ and $Ag_2S–P_2S_5$ glasses have been handicapped by relatively poor spectroscopic resolution, and the chemical shift ranges of the different $P^{(n)}$ units (see Fig. 1) in crystalline model compounds overlap rather strongly [8,9]. As a result, it has been impossible to address the question of binary versus statistical species distribution in such glasses and no conclusions have been available from these earlier works. It appears that in such systems, NMR observables other than chemical shifts must be utilized, for making reliable peak assignments. In the present paper we demonstrate that this task can be accomplished on the basis of indirect spin–spin (J-) couplings available by the application of two-dimensional NMR methods. As a matter of fact, J-based methods, such as homonuclear J-resolved [10] and INADE-QUATE [11] spectroscopies have been applied to various crystalline phosphates and a number of phosphate glasses in the past, giving useful information about both peak assignments and site connectivities [12–18]. To the best of our knowledge, however, no such applications to thiophosphate glasses have been reported and hence the structural picture in these systems remains unclear to the present date. As thiophosphate glasses show substantial promise for solid electrolyte applications in lithium ion battery systems [19–22], an improved understanding of their structural organization is important. Applying higher-speed ^{31}P MAS-NMR in conjunction with such J-based methods we give a quantitative structural description of nominally "stoichiometric" glasses with the compositions $NaPS_3$ and $AgPS_3$. As these glasses contain oxide impurities owing to their preparation processes, their compositions are more accurately described as $NaPS_{3-x}O_x$ and $AgPS_{3-x}O_x$. The $P^{(n)}$ distributions thus determined are discussed in relation to simple structural

* Corresponding author.
 E-mail address: eckerth@uni-muenster.de (H. Eckert).

scenarios defining the medium range structure of glassy thiophosphates.

2. Experimental

2.1. Sample preparation and characterization

Starting materials were P_2S_5 (ACROS, 99.9%, used as received), Ag_2S (ACROS, 99.9%) and anhydrous Na_2S, prepared via dehydration of the commercially available nonahydrate, by heating Na_2S $9H_2O$ (ACROS, chunks) for 12 h at 873 K and 10^{-4} bar, within a glassy carbon crucible that was placed into a stainless steel reactor. The glasses were prepared from the above three components in the desired molar ratios, within glassy carbon crucibles, which were quickly introduced for 10 min into a furnace pre-heated to 973 K that was situated in a nitrogen filled glovebox. After the melt initially settled, the temperature was raised to 1123 K and maintained for 20 min while the samples were being occasionally agitated. Following this treatment, the melts were rapidly quenched to room temperature between two copper plates under nitrogen atmosphere. All sample handling and preparations for MAS-NMR experiments were done in an Ar-filled glove box. To check for evaporation losses, the sample masses were recorded prior to and after sample melting. The total weight

Fig. 1. $P^{(n)}$ structural units present in thiophosphate glasses.

loss amounted to 2 ± 1 wt% for both glasses. Glass transition temperatures (onset points) were measured with a PERKIN ELMER—Pyris Diamond differential scanning calorimeter on 100 mg samples at a heating rate of 10 K/min. T_g was found to be 440 ± 5 K and 471 ± 5 K for $NaPS_3$ and $AgPS_3$ glass, respectively (see Fig. S1, Supplemental Materials Section). The value for $AgPS_3$ glass agrees with the literature value [9] within the limits of experimental error.

2.2. Solid state NMR.

^{31}P single pulse MAS NMR experiments were carried out on a BRUKER Avance 300 spectrometer at 121.44 MHz on a 7.1 T magnet and at spinning frequencies between 5.0 and 15.0 kHz. Typical acquisition parameters were: pulse lengths 3.5 µs (90° flip angle) and recycle delays 300 s. Chemical shifts are reported relative to 85% H_3PO_4. Signal deconvolutions into Gaussian components were done with the DMFIT software package [23]. Different phosphorus species were identified via homonuclear J-resolved spectroscopy. In this experiment, the amplitude modulation of the rotor synchronized spin echo due to $^2J(^{31}P–^{31}P)$ homonuclear indirect scalar coupling (damped by spin–spin relaxation) is recorded. Fourier transformation of the 2D time domain data set yields a spectrum exhibiting J-multiplets in the F_1 dimension. These data were measured at a spinning frequency of 15.0 kHz. Z-filtered spin echoes (one rotor period) were measured, incorporating a 32-step phase cycle [11]. The $\pi/2$ pulse lengths were around 3.5 µs. Depending on the sample, the rotor synchronized echoes were recorded for evolution times up to 100 ms corresponding to about 80 t_1 increments. For the 2D data processing, the States method was used to obtain pure absorption phase spectra. Data were recorded at a 30 s recycle delay, employing a saturation comb to ensure reproducible steady-state conditions.

The connectivity between different types of phosphorus units was further probed by two-dimensional refocused INADEQUATE experiments (see Fig. 2). This technique relies on double quantum filtering, based on homonuclear J-coupling, to yield correlation peaks between nuclei engaged in P–S–P linkages, whereas the signals from isolated ^{31}P nuclei are suppressed because the absence of J-coupling in them precludes the formation of double quantum coherences. These experiments were done at spinning rates of 15.0 kHz and $\pi/2$ pulse lengths near 3.5 µs. The DQ coherence buildup time 2τ was set to 6.25 ms, which is significantly shorter than the value on the order of 50 ms corresponding to $1/2J$ expected for maximum build-up. The t_1
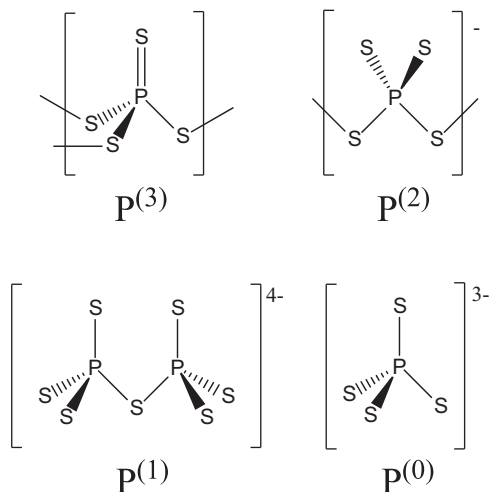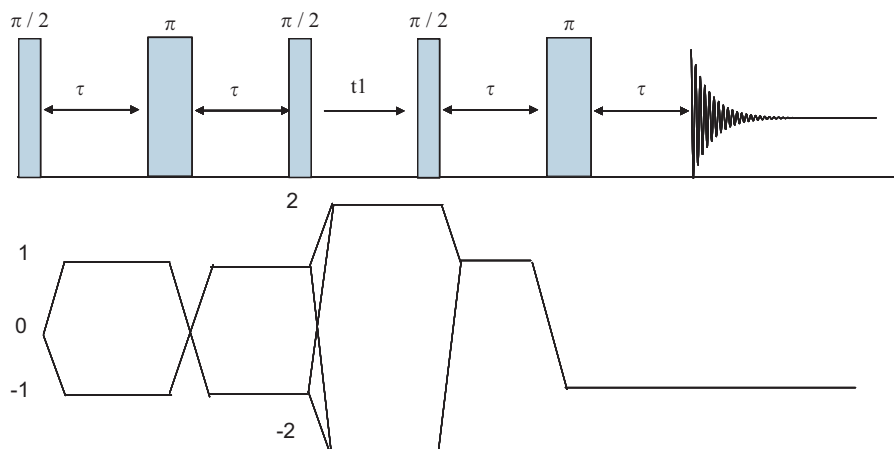

Fig. 2. Pulse scheme (top) and selected coherence transfer pathway (bottom) of the refocused INADEQUATE experiment.

increment was rotor synchronized to suppress spinning sideband artifacts. 32 scans were taken per t_1 increment and a total of 80 t_1 steps. The States method was used to obtain pure absorption phase spectra. The single-quantum background signals were eliminated by appropriate phase cycling. Both these pulse sequences were successfully optimized and tested on the model compound $Ag_7P_3S_{11}$ (see Fig. S2, Supplemental Materials Section). The asymmetric crystallographic unit of this compound possesses three distinct phosphorus atoms: an isolated orthothiophosphate (PS_4^{3-}) group at 103.3 ppm and the two crystallographically nonequivalent P atoms of a pyrothiophosphate ($P_2S_7^{4-}$) group at 91.9 and 101.1 ppm. The 2-D J-resolved spectrum yields the $^2J(^{31}P–^{31}P)$ coupling constant of 22.3 Hz, in excellent agreement with a previous measurement [24], and the refocused INADE-QUATE spectrum shows a complete suppression of the 103.3 ppm resonance.
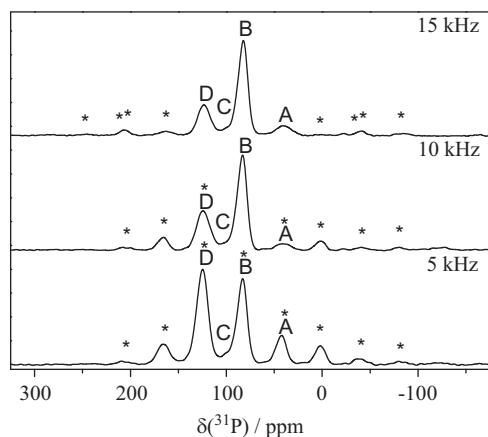
3. Results and discussion

Fig. 3 shows the ^{31}P MAS-NMR spectrum of glassy $NaPS_3$ at three different spinning frequencies. The spectrum observed with 5 kHz MAS shows close resemblance to data observed many years ago in glassy $LiPS_3$, obtained at similar spinning frequencies [8]. At that time, those spectra were interpreted as featuring a dominant $P^{(2)}$ species, and a set of spinning sidebands covering a wide frequency range was attributed to the sizeable chemical shift anisotropy of such $P^{(2)}$ units. Assuming that $LiPS_3$ and $NaPS_3$ glass are structurally analogous, Fig. 3 shows that this interpretation must be revised. Rather, the peak patterns observed in Ref. [8], and in an analogous fashion also for $AgPS_3$ glass in Ref. [9] represent superpositions of multiple resonances attributable to different $P^{(n)}$ species, with their associated spinning sideband profiles. While the spectra obtained at the spinning frequencies of 5 kHz, and even 10 kHz, cannot be interpreted without ambiguity, the situation becomes quite obvious at 15 kHz. Four distinct signal contributions (A–D) are clearly identified and their corresponding J-multiplicities are revealed in the 2D J-resolved spectrum, Fig. 4. The dominant resonance B at 83 ppm is clearly attributable to $P^{(2)}$ units based on its J-coupling triplet. The signal C at 96 ppm yields a doublet in the J-resolved spectrum, and thus must be assigned to $P^{(1)}$ units. Even though this signal is difficult to discern because of the relatively low concentration of these units, a J-doublet can be detected in the 2D J-resolved spectrum at enhanced contour levels (see Fig. S4, Supplemental Material). For species D near 123 ppm, the J-resolved spectrum reveals a quartet, indicating that this species must be assigned to $P^{(3)}$ units. Finally, species A at 40 ppm corresponds to a singlet, indicating the presence of monomeric $P^{(0)}$ units. The chemical shift of this unit does, however, not correspond to the chemical shifts normally observed for PS_4^{3-} groups in crystalline orthothiophosphates [8,9,25–28]. ^{31}P MAS-NMR studies on mixed lithium oxysulfide glasses and ceramics of the systems $[Li_2S]_{0.7}[(P_2O_5)_x(P_2S_5)_{1-x}]_{0.3}$ [25,26] and $[Li_3PO_4]_x[(Li_2S)_{0.6}(SiS_2)_{0.4}]_{1-x}$ [27–29] have observed multiple resonances near 84, 65, 34, and 8 ppm, respectively, which have been attributed to different possible monomeric $(PS_{4-n}O_n)^{3-}$ species. Assuming a monotonic dependence of ^{31}P chemical shifts on n, the resonance near

Fig. 3. 121.44 MHz ^{31}P MAS-NMR spectra of glassy $NaPS_3$ measured at three distinct spinning frequencies. Note that only at a spinning frequency of 15.0 kHz a clear identification of the MAS centerbands is possible. Spinning sidebands are indicated by asterisks.
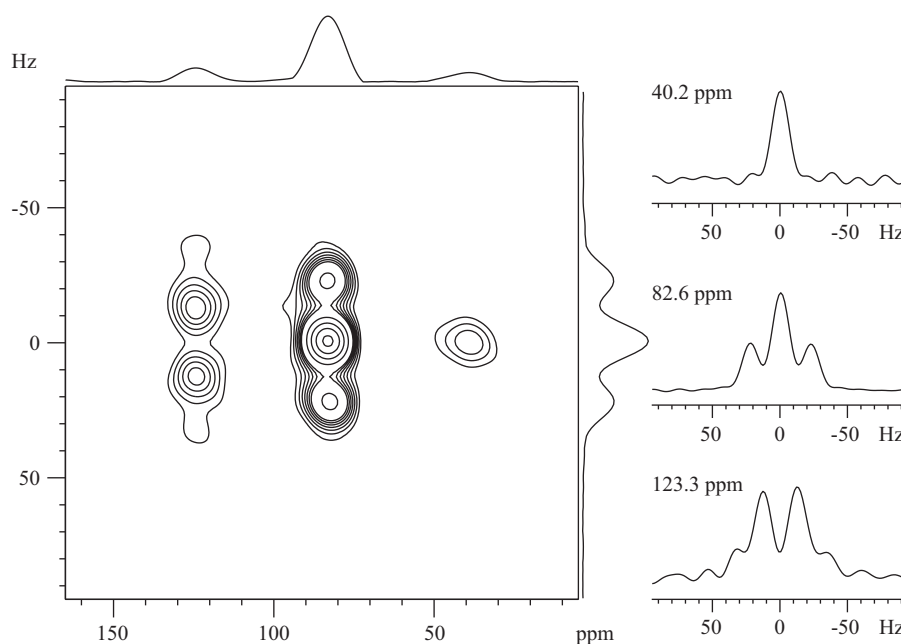

Fig. 4. J-resolved spectrum of glassy $NaPS_3$. Individual slices show the J-splitting patterns at the designated chemical shift values.

84 ppm was assigned to a superposition of the PS_4^{3-} and PS_3O^{3-} units, and the signals near 65, 34, and 8 ppm to $(PS_2O_2)^{3-}$, $(PSO_3)^{3-}$, and PO_4^{3-} groups, respectively [25–29]. Similar assignments were made previously for species identified in ^{31}P NMR spectra of aqueous extracts of $Na_2S–P_2S_5$ glasses [30]. Furthermore, the chemical shift of crystalline $\alpha–Na_3PO_3S$ was determined to be 33.4 ppm [31]. Comparison with these reference data then suggests that the signal at 40 ppm in the present glass most likely arises from PSO_3^{3-} units signifying the incorporation of some oxide into the glass. This incorporation might arise either from the use of starting materials containing some oxygen, from

oxygen incorporation during the synthesis, or from post-synthetic hydrolysis. Interestingly, we neither observe any evidence for mixed $P^{(1)}$, $P^{(2)}$ or $P^{(3)}$ units nor do we see multiple monomeric $PS_{4-n}O_n$ oxysulfide species. This result suggests that the PSO_3^{3-} unit formed has a particularly high stability in this system and serves as a "sink" for oxygen impurities.

Consistent with the assignment of the resonance at 40 ppm to a monomeric mixed species, this signal is completely screened out in the 2D INADEQUATE spectrum, which is shown for glassy $NaPS_3$ in Fig. 5.

Fig. 6 shows the spectral deconvolution of the ^{31}P MAS-NMR lineshape recorded at a spinning frequency of 15 kHz for the $NaPS_3$ glass. The corresponding lineshape parameters are summarized in Table 1. Analogous results have been included for the $AgPS_3$ glass for which the 2-D J-resolved spectrum is shown in Fig. 7. The comparison of these results for the $AgPS_3$ with the spectra of the $NaPS_3$ glass suggest analogous conclusions, except that the concentrations of the $P^{(1)}$ units are somewhat higher, and the chemical shift of the monomeric unit is found near 50 ppm. For $AgPS_3$ glass, the presence of some $P^{(1)}$ units besides the dominant $P^{(2)}$ species had already been detected in the 5 kHz MAS-NMR study, suggesting already a sizeable deviation from the binary species distribution model [9]. However, no evidence for $P^{(3)}$ or $P^{(0)}$ units was observable in that study. Since the low-speed spectra of Fig. 3 match the ones published earlier rather closely, we suspect that both the $P^{(3)}$ species D and the monomeric mixed oxysulfide species A were also present in the samples studied in Refs. [8,9]. Consequently, it is now clear from these data that the binary species distribution model is not applicable to alkali and silver thiophosphate glasses and alternate models need to be considered.
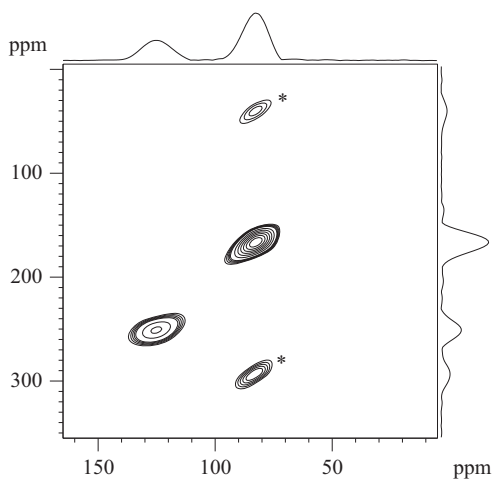

Fig. 5. 2D INADEQUATE spectrum of glassy $NaPS_3$. Spinning sidebands are indicated by asterisks.
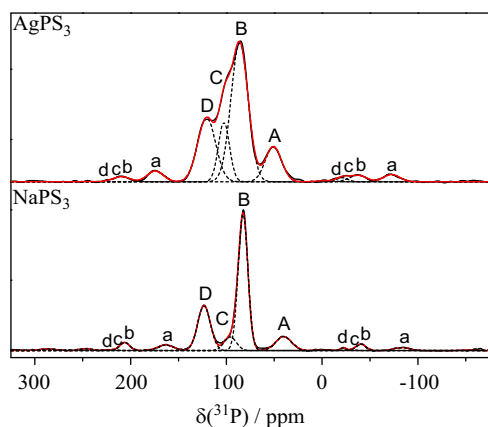

Fig. 6. Deconvolution of the ^{31}P MAS-NMR spectra of glassy $AgPS_3$ and $NaPS_3$. The labels A, B, C, and D identify the four distinct MAS centerbands. The corresponding spinning sidebands are indicated by small letters.
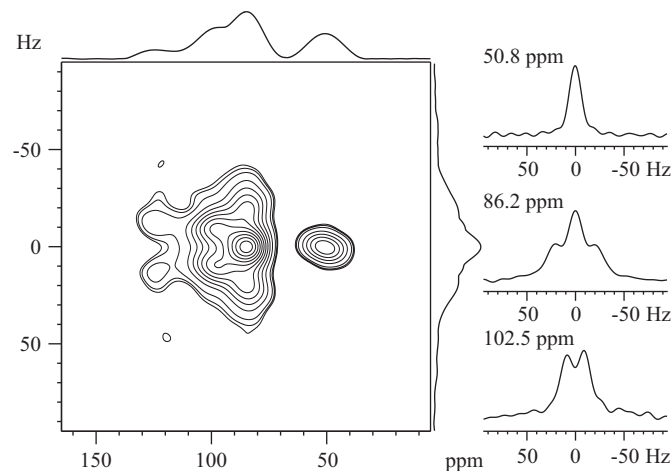

Fig. 7. J-resolved spectrum of glassy $AgPS_3$. Individual slices show the J-splitting patterns at the designated chemical shift values.
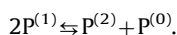
Table 1
^{31}P chemical shifts, line widths, area fractions, J-splitting patterns, and $^2J(^{31}P–^{31}P)$ spin spin coupling constants observed via 2D J-resolved spectroscopy in glassy $NaPS_3$ and $AgPS_3$.

Glass comp.	$P^{(n)}$	δ (± 0.3) (ppm)	Δ (± 0.5) (ppm)	G/L	Area fraction (± 3) (%)	J-splitting pattern	$^2J(^{31}P–^{31}P)$ (± 1.0) (Hz)
$NaPS_3$	$P^{(0)}$ (A)	40.2	19.8	1.0	13.0	Singlet	–
	$P^{(2)}$ (B)	82.6	11.9	1.0	56.3	Triplet	22.5
	$P^{(1)}$ (C)	96.0	15.0	1.0	7.2	Doublet	ca. 21
	$P^{(3)}$ (D)	123.3	15.6	1.0	23.5	Quartet	ca. 25
$AgPS_3$	$P^{(0)}$ (A)	50.8	19.9	1.0	16.2	Singlet	–
	$P^{(2)}$ (B)	86.2	21.0	1.0	48.3	Triplet	22.1
	$P^{(1)}$ (C)	102.5	13.8	1.0	13.5	Doublet	17.0
	$P^{(3)}$ (D)	120.6	22.0	1.0	22.0	Quartet	ca. 25

Table 1 summarizes the species distributions obtained from quantitative peak deconvolutions. Based on these numbers we can calculate the average negative charge per phosphorus atom, n_P, for both glasses. According to the designated metathiophosphate glass composition a n_P value of one is expected. We find slightly higher values, $n_P = 1.10$ and 1.25 for glassy NaPS$_3$ and glassy AgPS$_3$, respectively. This deviation might be a direct or indirect consequence of the oxide incorporation into these glasses. Evaluation of the data in Table 1, assuming the new species to be PSO$_3^{3-}$ groups, indicates that 13% of the sulfur atoms in glassy NaPS$_3$ are replaced by oxygen, corresponding to a formula NaPS$_{2.61}$O$_{0.39}$. In glassy AgPS$_3$ 16% of sulfur are replaced by oxygen, corresponding to a formula AgPS$_{2.52}$O$_{0.48}$. These sulfur losses would correspond to weight deficits of 4% and 3% in NaPS$_3$ and AgPS$_3$, respectively. As these numbers are somewhat larger than the experimentally observed weight losses of 2%, it is conceivable that the sulfur liberated by oxygen replacement is not all lost in the vapor phase, but in part retained in the melt in the form of additional chalcogen bridges or S–S linkages.

Overall, the results of the present study show that the structural organization of oxide-containing sodium and silver thiophosphate glasses differs fundamentally from those of the analogous oxidic glasses. While the NaPO$_3$ and AgPO$_3$ networks closely adhere to the binary model, (i.e., P$^{(2)}$ units are the sole species present), these oxy-chalcogenide glasses feature all four possible P$^{(n)}$ units, from P$^{(0)}$ to P$^{(3)}$ at sizeable concentrations (see Table 1). The oxide impurities appear, however, only in the monomeric species. In Fig. 8 we compare these P$^{(n)}$ concentrations with predicted values based on a binomial statistical distribution of the total charge dispersed over the network. The comparison with the experimental data suggests that the binomial model may be a good approximation of the situation encountered in reality, with one important exception: P$^{(1)}$ species appear to be strongly under-represented in the glassy state, indicating that they have relatively low stabilities, while the concentrations of P$^{(0)}$ and P$^{(2)}$ units are higher than expected from the statistical model. These discrepancies might arise from a "disproportionation" reaction according to a melt equilibrium of the type:

$$2P^{(1)} \leftrightarrows P^{(2)} + P^{(0)}.$$

Based on this interpretation, Table 1 suggests that the positive counterion (Ag$^+$ vs. Na$^+$) has a strong influence on this equilibrium, the K-value being significantly higher for NaPS$_3$ glass than for AgPS$_3$ glass. In addition, we suspect that this disproportionation equilibrium may be influenced by the presence of oxide impurities in the present samples.

Finally, it is interesting to see that the 2D INADEQUATE spectrum of NaPS$_3$ glass is completely dominated by auto-correlations, see Fig. 5. While the absence of any observable cross-peaks linking the P$^{(3)}$ and P$^{(2)}$ or the P$^{(2)}$ and P$^{(1)}$ resonances
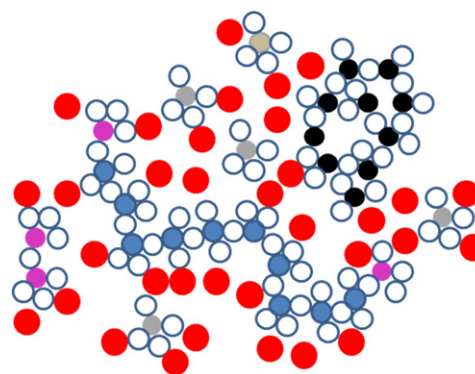
Fig. 9. Schematic description of the heterogeneous structure of NaPS$_3$ and AgPS$_3$ glasses: P atoms of P$^{(0)}$, P$^{(1)}$, P$^{(2)}$, and P$^{(3)}$ units are depicted by gray, purple, blue and black circles, sulfur (or oxygen) atoms are shown by open circles, and sodium or silver atoms by red circles. (For interpretation of the references to color in this figure legend, the reader is referred to the web version of this article.)

does not prove the complete absence of such linkages, the data do suggest that such connectivities are under-represented in these glasses. Our failure of observing P$^{(1)}$–P$^{(2)}$ connectivities in these glasses may be a consequence of the rather low P$^{(1)}$ species concentrations, but the absence of detectable P$^{(2)}$–P$^{(3)}$ connectivities implies a rather inhomogeneous and segregated structure. Fig. 9 presents a qualitative structural model accounting for these data. While chains of metathiophosphate units are the dominant feature, the structure also contains some dimeric pyrothiophosphate (P$^{(1)}$), and monomeric orthothiophosphate (P$^{(0)}$) species interacting with the cations. The latter evidently incorporate oxygen impurities, leading to the preferential formation of oxy-thiophosphate units. Based on the INADEQUATE results the P$^{(3)}$ species are mostly connected among themselves, forming electrically neutral molecular and/or segregated polymeric structures. This kind of molecular-level segregation which is also characteristic of binary phosphorus–sulfur glasses [32] portrays a rather inhomogeneous nanostructure of these materials. In spite of these findings, the differential scanning calorimetry plots give no indication of macroscopic phase separation.

4. Conclusions

In summary, the present study illustrates the power and potential of J-coupling based spectral editing methods for analyzing the P$^{(n)}$ species distributions in sodium and silver metathiophosphate glasses containing oxygen impurities. In both glasses these distributions as extracted from ^{31}P MAS-NMR data are found to be close to those predicted by a binomial distribution, with an important modification concerning a lower-than-expected occurrence of P$^{(1)}$ units, which might be due to a disproportionation reaction into P$^{(0)}$ and P$^{(2)}$ species. The species distribution is completely different from that encountered in simple alkali metaphosphate glasses, which follow the binary model. Also, in contrast to phosphate glasses, the one- and two-dimensional spectra of these thiophosphates suggest that their structures are rather inhomogeneous and segregated at the molecular level.
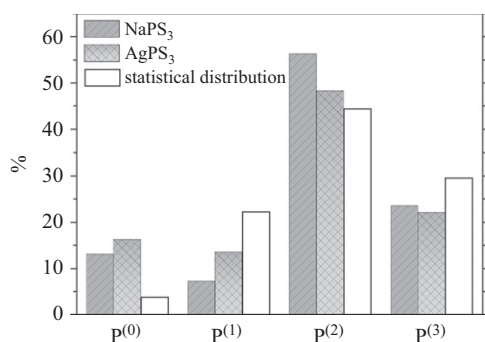
Fig. 8. P$^{(n)}$ population distributions in NaPS$_3$ and AgPS$_3$ glasses, and comparison with the predicted distribution based on binomial statistics.

Appendix A. Supplementary Material

Supplementary data associated with this article can be found in the online version at http://dx.doi.org/10.1016/j.ssnmr.2012.05.0011.

References

[1] A.R. Grimmer, J. Chim Phys. 89 (1992) 413.
[2] A.K. Cheetham, N. Clayden, C.M. Dobson, R. Jakeman, J. Chem. Soc. Chem. Commun. (1986) 195.
[3] G.L. Turner, A. Smith, R.J. Kirkpatrick, E. Oldfield, J. Magn. Reson. 70 (1986) 408.
[4] P. Mustarelli, Phosphorus Res. Bull. 10 (1999) 25.
[5] H. Eckert, Prog. Nucl. Magn. Reson. Spectrosc. 23 (1992) 159, and references therein.
[6] R.K. Brow, R.J. Kirkpatrick, G.L. Turner, J. Non-Cryst. Solids 116 (1990) 39.
[7] J.R. Van Wazer, J. Am. Chem. Soc. 72 (1950) 644.
[8] H. Eckert, Zh. Zhang, J.H. Kennedy, Chem. Mater. 2 (1990) 273.
[9] Zh. Zhang, J.H. Kennedy, H. Eckert, J. Am. Chem. Soc. 114 (1992) 5775.
[10] S.P. Brown, M. Pérez-Torralba, D. Sanz, R.M. Claramunt, L. Emsley, L. Chem. Commun. 7 (2002), 1852.
[11] L. Duma, W.C. Lai, M. Carravetta, L. Emsley, S.P. Brown, M.H. Levitt, Chem. Phys. Chem. 5 (2004) 815.
[12] A. Lesage, M. Bardet, L. Emsley, J. Am. Chem. Soc. 121 (1999) 10987.
[13] P. Guerry, M.E. Smith, S.P. Brown, J. Am. Chem. Soc. 131 (2009) 11861.
[14] X. Helluy, C. Marichal, A. Sebald, J. Phys. Chem. B 104 (2000) 2836.
[15] F. Fayon, D. Massiot, M.H. Levitt, J.J. Titman, D.H. Gregory, L. Duma, L. Emsley, S.P. Brown, J. Chem. Phys. 122 (2005) 194313.
[16] F. Fayon, I.J. King, R.K. Harris, J.S.O. Evans, D. Massiot, Compt. Rend. Chim. 7 (2004) 351.
[17] S.H. Santagneli, C.C. de Araujo, W. Strojek, H. Eckert, G. Poirier, S.J.L. Ribeiro, Y. Messaddeq, J. Phys. Chem. B 111 (2007) 10109.
[18] C.C. de Araujo, W. Strojek, L. Zhang, H. Eckert, G. Poirier, S.J.L. Ribeiro, Y. Messaddeq, J. Mater. Chem. 16 (2006) 3277.
[19] K. Minami, Solid State Ionics 192 (2011) 122.
[20] F. Mizuno, A. Hayashi, K. Tadanaga, M. Tatsumisago, Solid State Ionics 177 (2006) 2721.
[21] H.J. Deiseroth, S.T. Kong, H. Eckert, J. Vannahme, C. Reiner, T. Zaiß, M. Schlosser, Angew. Chem. Int. Ed. 47 (2008) 755.
[22] S.T. Kong, Ö. Gün, B. Koch, H.J. Deiseroth, H. Eckert, C. Reiner, Chem. Eur. J. 16 (2010) 5138.
[23] D. Massiot, F. Fayon, M. Capron, I. King, S.L. Calve, B. Alonso, J.O. Durand, B. Bujoli, Z. Gan, G. Hoatson, Magn. Reson. Chem. 40 (2002) 70.
[24] J. Schmedt auf der Günne, Ph. D. Thesis, Münster, 2000.
[25] K. Minami, F. Mizuno, A. Hayashi, M. Tatsumisago, J. Non-Cryst. Solids 354 (2008) 370.
[26] A. Hayashi, R. Araki, K. Tadanaga, M. Tatsumisago, T. Minami, Phys. Chem. Glasses 40 (1996) 487.
[27] M. Tatsumsisago, H. Yamashita, A. Hayashi, H. Morimoto, T. Minami, J. Non-Cryst. Solids 274 (2000) 30.
[28] A. Hayashi, R. Araki, K. Tadanaga, M. Tatsumisago, T. Minami, Phys. Chem. Glasses 40 (1999) 140.
[29] K. Hirai, M. Tatsumisago, M. Takahashi, T. Minami, J. Am. Ceram. Soc. 79 (1996) 349.
[30] L. Maier, J.R. van Wazer, J. Am. Chem. Soc. 84 (1962) 3054.
[31] M. Pompetzki, L. van Wüllen, M. Jansen, Z. Anorg. Allg. Chem. 630 (2004) 384.
[32] M. Tullius, D. Lathrop, H. Eckert, J. Phys. Chem. 93 (1990) 2145.